PHYSICAL REVIEW D **85,** 051502(R) (2012)

Exclusive production of quarkonia as a probe of the generalized parton distribution for gluons

John Koempel,[1] Peter Kroll,[2,3] Andreas Metz,[1] and Jian Zhou[3]
[1]*Department of Physics, Barton Hall, Temple University, Philadelphia, Pennsylvania 19122, USA*
[2]*Fachbereich Physik, Universität Wuppertal, 42097 Wuppertal, Germany*
[3]*Institut für Theoretische Physik, Universität Regensburg, 93040 Regensburg, Germany*
(Received 21 December 2011; published 16 March 2012)

Exclusive quarkonium photo- and electro-production off the nucleon is studied in the framework of generalized parton distributions (GPDs). The short-distance part of the process is treated at leading order in perturbative Quantum Chromodynamics. The main focus is on the GPD E for gluons. On the basis of different models for E^g we estimate the transverse target spin asymmetry for typical kinematics of a future Electron Ion Collider. We also explore the potential of measuring the polarization of the recoil nucleon.

DOI: 10.1103/PhysRevD.85.051502 PACS numbers: 12.38.−t, 12.39.St, 13.60.Le, 13.88.+e

I. INTRODUCTION

For about 15 years, GPDs [1–9] have been playing a key role in hadronic physics for a number of reasons. First, GPDs serve as unifying objects, containing the information encoded both in ordinary parton distributions and in form factors. Second, GPDs allow us to explore the partonic structure of hadrons in three dimensions [10–13]. Third, GPDs enter Ji's spin sum rule of the nucleon [2].

GPDs can be measured in hard exclusive processes like deep-virtual Compton scattering off the nucleon or hard exclusive meson production [2–5,14,15]. They depend on three kinematical variables: the average momentum fraction x of the partons, the longitudinal momentum transfer ξ to the nucleon (skewness), and the invariant momentum transfer t of the process, i.e., $F = F(x, \xi, t)$ for a generic GPD F. According to [2], GPDs give access to the angular momenta of quarks and gluons inside the nucleon, where the total spin of the nucleon is given by $\frac{1}{2} = \sum_q J^q + J^g$. Specifically, the gluon angular momentum can be determined through [2]

$$J^g = \frac{1}{2}\int_0^1 dx[H^g(x, \xi, 0) + E^g(x, \xi, 0)], \qquad (1)$$

with H^g and E^g denoting the dominant (leading twist) GPDs of unpolarized gluons inside the nucleon. Considerable information on H^g is already available, for it is connected to the ordinary unpolarized gluon distribution via $H^g(x, 0, 0) = xg(x)$—see for instance Refs. [16–22]. In comparison, our knowledge about E^g is still marginal. Therefore, in particular, the value for J^g in Eq. (1) is still very uncertain.

It has been known for quite some time that exclusive quarkonium (J/ψ or Υ) production off the nucleon is very suitable for probing the gluonic structure of the nucleon in a clean way [23,24], since quark exchange plays only a minor role. Moreover, due to the large scale provided by the heavy quark/meson mass, perturbative Quantum Chromodynamics (QCD) can be applied even for photo-production. In the present work, we consider both photo- and electro-production of J/ψ and Υ off a proton target. Using leading order (LO) results for the hard scattering coefficients we study the prospects for measuring E^g by means of quarkonium production. To this end we consider several models for E^g, and compute the transverse target spin asymmetry as well as a double-spin observable which requires polarimetry of the recoil nucleon. We provide numerical results for typical kinematics of a potential future Electron Ion Collider (EIC) [25–27].

II. THEORETICAL FRAMEWORK

For definiteness, we consider the process

$$\gamma^{(*)}(q, \mu) + p(p, \nu) \to V(q', \mu') + p(p', \nu'), \qquad (2)$$

where the 4-momenta and the helicities of the particles are specified. We further use $Q^2 = -q^2$, $m^2 = p^2 = p'^2$, $m_V^2 = q'^2$, $t = (p - p')^2$, and the squared photon-nucleon cm energy $W^2 = (p + q)^2$. The skewness variable can be expressed as

$$\xi = \frac{\tilde{x}_B}{2 - \tilde{x}_B}, \quad \text{with} \quad \tilde{x}_B = \frac{m_V^2 + Q^2}{W^2 + Q^2}, \qquad (3)$$

which holds for arbitrary values of Q^2. The minimal value of t is given by $|t_0| = 4m^2\xi^2/(1 - \xi^2)$.

For Q^2 much larger than all other scales of the process, an all order proof of QCD factorization has been formulated for the process in (2) [14]. In the case of quarkonium production, one may expect factorization to hold for arbitrary Q^2. In fact, a next-to-leading order (NLO) calculation of the unpolarized photo-production cross section is compatible with factorization [28].

To LO in the strong coupling there are six Feynman graphs—see Fig. 1 for a sample diagram. They factorize into the hard subprocess $\gamma^* g \to Vg$ and gluon GPDs. We computed the helicity amplitudes of the subprocess in the nonrelativistic approximation for which the heavy quark and antiquark carry the same momentum. Our results agree with previous calculations [28–30]. The structure of the

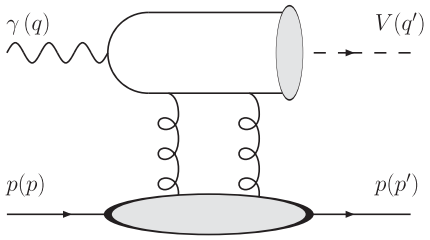

FIG. 1. Sample LO diagram for the process in (2). The lower part of the diagram is parameterized in terms of gluon GPDs.

LO amplitudes implies that one is sensitive only to the GPDs H^g and E^g [29,30].

For transversely polarized photons and vector mesons, the nonzero helicity amplitudes $\mathcal{M}_{\mu'\nu',\mu\nu}$ of the full process read

$$\mathcal{M}_{\pm+,\pm+} = \mathcal{M}_{\pm-,\pm-} = C\sqrt{1-\xi^2}\langle H^g_{\text{eff}}\rangle, \tag{4}$$

$$\mathcal{M}_{\pm-,\pm+} = -\mathcal{M}_{\pm+,\pm-} = -C\frac{\sqrt{-t'}}{2m}\langle E^g\rangle, \quad \text{with}$$
$$\langle F\rangle = \int_0^1 \frac{dx}{(x+\xi)(x-\xi+i\varepsilon)} F(x,\xi,t) \tag{5}$$

for a generic GPD F. In Eqs. (4) and (5), we use the definitions $H^g_{\text{eff}} = H^g - \xi^2/(1-\xi^2)E^g$, $t' = t - t_0$, and $C = 16\pi e_q e \alpha_s f_V m_V/(N_c(Q^2+m_V^2))$, where f_V denotes the quarkonium decay constant. Moreover, one has

$$\mathcal{M}_{0\nu',0\nu} = -\frac{Q}{m_V}\mathcal{M}_{\pm\nu',\pm\nu} \tag{6}$$

for longitudinal transitions. A corresponding relation between the longitudinal and the transverse amplitudes was previously obtained in the pioneering work on exclusive J/ψ production in the leading double-log approximation [23].

III. GENERALIZED PARTON DISTRIBUTIONS

For the GPD H we take the parameterizations obtained in previous analyses [18,20]. Note that quark GPDs are also needed since the GPDs are evolved to different scales. In the case of E, we use the valence quark distributions from Ref. [31,32], while we explore different scenarios for gluons and sea quarks. They are modeled through double distributions [1,33] according to

$$E^i(x,\xi,t) = \int_{-1}^1 d\beta \int_{-1+|\beta|}^{1-|\beta|} d\alpha \delta(\beta+\xi\alpha-x) f^i(\beta,\alpha,t),$$
$$f^i(\beta,\alpha,t) = E^i(\beta,0,t)\frac{15}{16}\frac{[(1-|\beta|)^2-\alpha^2]^2}{(1-|\beta|)^5}, \quad \text{with}$$
$$E^i(\beta,0,t) = e^{b_e t}|\beta|^{-\alpha'_e t}E^i(|\beta|,0,0). \tag{7}$$

For gluons we define $xe^g(x) \equiv E^g(x,0,0)$ (with an extra factor x as for H^g) and investigate the two cases

$$e^g(x) = N^g x^{-1-\delta_e}(1-x)^{\beta^g_e}, \tag{8}$$

$$e^g(x) = N^g x^{-1-\delta_e}(1-x)^{\beta^g_e}\tanh(1-x/x_0), \tag{9}$$

where the ansatz in (9) has a node at $x = x_0$. Such a possibility is currently not ruled out [34]. We further define $e^q(x) \equiv E^q(x,0,0)$, and use a flavor-symmetric sea, i.e., $e^{\bar q} \equiv e^{\bar u} = e^{\bar d} = e^{\bar s} = e^s$. For $e^{\bar q}(x)$ we make an ansatz analogous to (8) and do not consider a node. For the parameters b_e, α'_e, and δ_e we do not distinguish between gluons and sea quarks.

Two constraints have to be satisfied when fixing the parameters for e^g and $e^{\bar q}$. First, the momentum sum rule for unpolarized parton distributions in combination with Ji's spin sum rule leads to

$$e^g_{20} = -\sum_q e^{q_{\text{val}}}_{20} - 2\sum_q e^{\bar q}_{20}, \quad \text{with} \tag{10}$$

$$e^i_{n0} \equiv \int_0^1 dx x^{n-1} e^i(x). \tag{11}$$

Second, the density interpretation of GPDs in the impact parameter space [13] leads to a positivity bound for e^g and $e^{\bar q}$ —see Refs. [19,30–32] for more details. In particular, one finds $b_e < b_h$, $\alpha'_e \le \alpha'_h$, where b_h and α'_h appear in the double distribution ansatz of H^g. We take $b_h = 2.58\ \text{GeV}^{-2} + 0.25\ \text{GeV}^{-2}\ln\frac{m^2}{m^2+\mu^2}$ (with μ representing the scale of the GPD) and $\alpha'_h = 0.15$ from previous work [18,20]. We choose $b_e = 0.9 b_h$ in order to respect a positivity bound, and explore two different values for α'_e (see Table I). Moreover, we use $\delta^e = 0.1$, as well as $\beta^g_e = 6$ and $\beta^{\bar q}_e = 7$ [32]. (Note that the parameters δ^e and α'_e correspond to the hard Pomeron trajectory measured in vector meson electro-production.) After these choices have been made, only the normalization constants N^g and $N^{\bar q}$ remain to be determined.

We parameterize e^g and $e^{\bar q}$ at the scale $\mu = 2$ GeV. For e^g we consider five different variants, where the respective

TABLE I. Parameters of e^g and $e^{\bar q}$ at the scale $\mu = 2$ GeV. For gluons, the Variants 1, 2, 3 refer to the ansatz in (8), while Variants 4, 5 refer to (9). Also shown is the second moment e^g_{20}, and values for the angular momenta as defined in (1).

Variants	α'_e	N^g	x_0	e^g_{20}	J^g	$N^{\bar q}$	J^s
1	0.15	0		0	0.214	−0.009	0.014
2	0.15	−0.878		−0.164	0.132	0.156	0.041
3	0.10	−1.017		−0.190	0.119	0.182	0.045
4	0.10	3.015	0.05	−0.190	0.119	0.182	0.045
5	0.10	−1.974	0.3	−0.190	0.119	0.182	0.045

parameters are listed in Table I. Variant 1 means $e^g = 0$, and the normalization $N^{\bar{q}}$ is fixed by means of the relation in (10). (There is actually some support for a rather small E^g: this GPD has a model-dependent relation to the transverse momentum dependent gluon Sivers function [35], which may be small [36–38].) In the remaining four cases we first determine $N^{\bar{q}}$ by saturating the positivity bound, then compute N^g from (10), and finally check whether e^g satisfies the positivity bound. Variants 4 and 5 for e^g contain a node. The positivity bound does not allow one to fix the sign of $N^{\bar{q}}$. However, none of our general conclusions depends on this sign [30]. We also checked that all variants for e^g and $e^{\bar{q}}$ are compatible with a preliminary data point for the transverse target spin asymmetry for exclusive ϕ production from HERMES [30,39]. When calculating observables we evolve the GPDs to the scale $\mu = (m_V^2 + Q^2)^{1/2}$ by using the code of Vinnikov [40]. In Fig. 2, the GPDs are displayed at the scale of the quarkonium masses.

We stress that, in general, the model-independent constraints on e^g and $e^{\bar{q}}$ are rather loose. Therefore, we consider a number of examples in order to demonstrate how the spin asymmetries may look. We also explore the possibility of a node in e^g which allows for a rather different value for the convolution with the hard subprocess amplitude without changing the second moment. The chosen positions of the node are again to be viewed as possible scenarios.

Following [2], the gluon and strange quark contributions to the nucleon spin are $J^g = (h^g_{20} + e^g_{20})/2$ as well as $J^s = (h^s_{20} + e^s_{20})$, where the densities $h^{g/q}$ are related to $H^{g/q}$ in the same way as $e^{g/q}$ are related to $E^{g/q}$. Taking $h^g_{20} = 0.4276$ and $h^s_{20} = 0.0153$ from [32,41] leads to the values for J^g and J^s in Table I. Because of (10), a change of J^s implies a change of J^g. For our parameterizations, the contribution from E^g to the nucleon spin can be significant (up to about 20%).

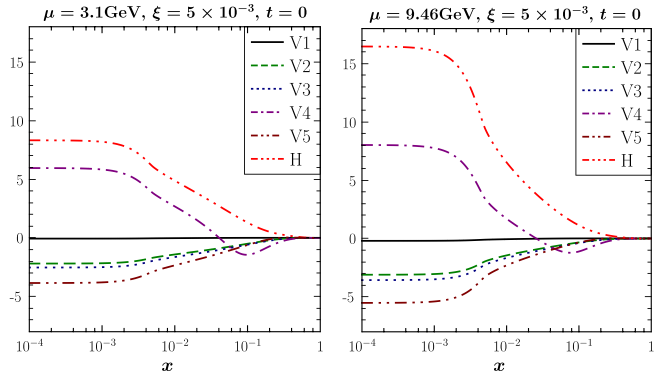

FIG. 2 (color online). Variants 1–5 for E^g, together with H^g, at the scales $\mu = m_{J/\psi} = 3.1$ GeV (left) and $\mu = m_\Upsilon = 9.46$ GeV (right).

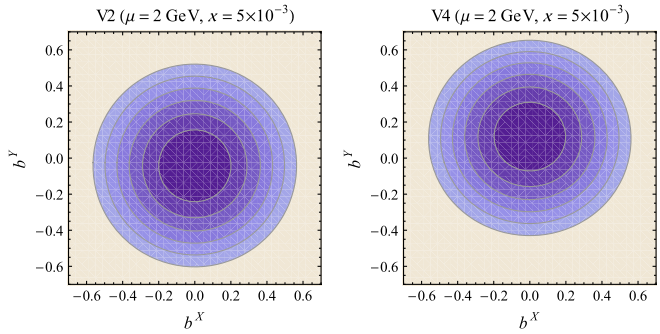

FIG. 3 (color online). Density in (12) for Variant 2 (left) and Variant 4 (right) at $x = 0.005$ and $\mu = 2$ GeV. The outer ring indicates half of the maximum density.

One can also calculate the density of unpolarized gluons in transverse position (impact parameter $b_\perp$) space. If the nucleon is transversely polarized (along the X-direction), this density is given by [13]

$$\mathcal{H}^{g,X}(x, \vec{b}_\perp) = \mathcal{H}^g(x, \vec{b}_\perp^2) - \frac{b_\perp^Y}{m} \frac{\partial}{\partial \vec{b}_\perp^2} \mathcal{E}^g(x, \vec{b}_\perp^2), \quad (12)$$

with $\mathcal{H}^g$ and $\mathcal{E}^g$ denoting the $b_\perp$-space representation of H^g and E^g, respectively. The sample plots in Fig. 3 show, in particular, how much the maximum of the density in (12) is shifted away from the origin due to the presence of the E^g-term.

IV. POLARIZATION OBSERVABLES.

As discussed in Sec. II, one has two independent amplitudes: the non-flip amplitude $\mathcal{M}_{++,++}$, dominated by H^g, and the spin-flip amplitude $\mathcal{M}_{+-,++}$, which is determined by E^g. The following observables allow one to measure those amplitudes (up to an overall phase): the unpolarized cross section, the transverse target single spin asymmetry (SSA) A_N (with the polarization being normal to the reaction plane—often A_N is also denoted as A_{UT}), and two double spin asymmetries (DSAs) requiring a polarized

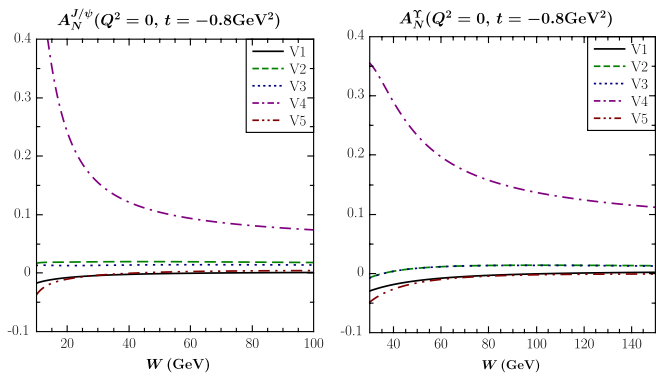

FIG. 4 (color online). SSA A_N in (13) for photo-production of J/ψ (left) and Υ (right) as function of W for different variants of E^g.

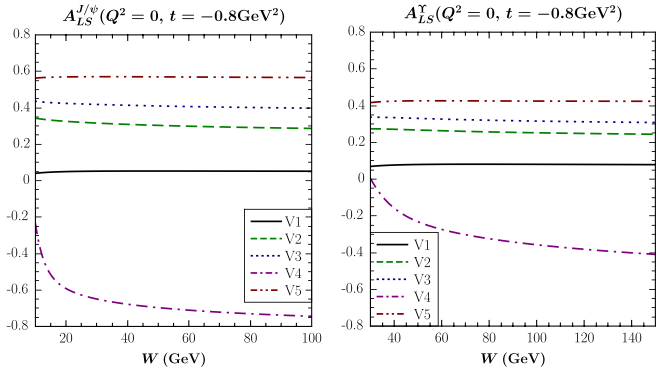

FIG. 5 (color online). DSA A_{LT} in (14) for photo-production of J/ψ (left) and Υ (right) as function of W for different variants of E^g.

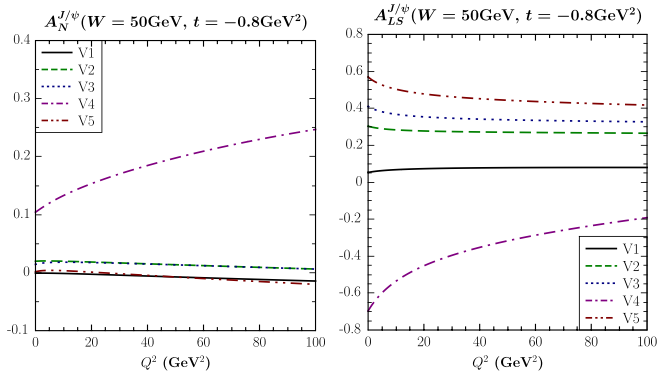

FIG. 6 (color online). A_N (left) and A_{LS} (right) for production of J/ψ as function of Q^2 for different variants of E^g.

target and polarimetry of the recoil nucleon [30]. Here we focus on

$$A_N = \frac{-2\,\mathrm{Im}(\mathcal{M}_{++,++}\mathcal{M}^*_{+-,++})}{|\mathcal{M}_{++,++}|^2 + |\mathcal{M}_{+-,++}|^2}, \tag{13}$$

$$A_{LS} = \frac{2\,\mathrm{Re}(\mathcal{M}_{++,++}\mathcal{M}^*_{+-,++})}{|\mathcal{M}_{++,++}|^2 + |\mathcal{M}_{+-,++}|^2}, \tag{14}$$

where for the DSA A_{LS} the target is longitudinally polarized, and the outgoing nucleon is transversely polarized (in the reaction plane, ''sideways'') [30]. We consider production of both J/ψ and Υ for typical EIC kinematics. While the J/ψ final state has a larger cross section, one can expect a better convergence of the α_s-expansion in the case of the Υ [28]. A detailed comparison with existing data for the unpolarized cross section will be given elsewhere [30]—see also Ref. [28].

In Fig. 4, A_N is shown for photo-production of J/ψ and Υ as a function of W. This asymmetry is rather small for most variants of E^g, mainly because the respective non-flip amplitude and the spin-flip amplitude have a similar phase. It can also be seen, however, that larger values of A_N are currently not ruled out. On the basis of a LO calculation one can not draw a definite conclusion about the optimal W for a measurement of A_N. But higher-order terms to the unpolarized cross section are better under control for lower values of W [28]. In general, the spin asymmetries are less influenced by NLO corrections than the cross section [30]. The DSA A_{LS} is displayed in Fig. 5. This observable is small only if E^g is small. It is worthwhile to explore the feasibility of a corresponding measurement, since A_{LS} may give the most direct access to E^g. (We note that, from a theoretical point of view, the DSA A_{SL} is equally well suited [30].) Finally, the Q^2-dependence of A_N and A_{LS} for J/ψ production is shown in Fig. 6. Electro-production at low Q^2 is attractive because of the large count rates. For $Q^2 \geq m_V^2$, higher-order corrections may be less important [28], but an explicit calculation does not yet exist.

V. SUMMARY

We have explored the potential of measuring the GPD E^g through exclusive production of quarkonium at a future Electron Ion Collider. The study is based on a LO calculation of the short-distance part of the process, and several models for E^g which respect the currently known constraints. Most variants of E^g lead to a rather small transverse target SSA A_N, but a healthy A_N is presently not ruled out either. We have also found promising results for a double polarization observable (polarized target and polarized recoil nucleon), which provides a quite direct access to E^g.

ACKNOWLEDGMENTS

We thank Markus Diehl, Zein-Eddine Meziani, and Feng Yuan for useful discussions and encouragement. This work was supported in part by the BMBF under the Contract No. 06RY258, and the NSF under the Grant No. PHY-0855501.

[1] D. Mueller *et al.*, Fortschr. Phys. **42**, 101 (1994).
[2] X. D. Ji, Phys. Rev. Lett. **78**, 610 (1997).
[3] A. V. Radyushkin, Phys. Lett. B **380**, 417 (1996).
[4] A. V. Radyushkin, Phys. Lett. B **385**, 333 (1996).
[5] X. D. Ji, Phys. Rev. D **55**, 7114 (1997).
[6] K. Goeke, M. V. Polyakov, and M. Vanderhaeghen, Prog. Part. Nucl. Phys. **47**, 401 (2001).
[7] M. Diehl, Phys. Rep. **388**, 41 (2003).

[8] A. V. Belitsky and A. V. Radyushkin, Phys. Rep. **418**, 1 (2005).
[9] S. Boffi and B. Pasquini, Riv. Nuovo Cimento **30**, 387 (2007).
[10] M. Burkardt, Phys. Rev. D **62**, 071503 (2000).
[11] J. P. Ralston and B. Pire, Phys. Rev. D **66**, 111501 (2002).
[12] M. Diehl, Eur. Phys. J. C **25**, 223 (2002).
[13] M. Burkardt, Int. J. Mod. Phys. A **18**, 173 (2003).
[14] J. C. Collins, L. Frankfurt, and M. Strikman, Phys. Rev. D **56**, 2982 (1997).
[15] J. C. Collins and A. Freund, Phys. Rev. D **59**, 074009 (1999).
[16] L. Frankfurt, M. Strikman, and C. Weiss, Annu. Rev. Nucl. Part. Sci. **55**, 403 (2005).
[17] S. V. Goloskokov and P. Kroll, Eur. Phys. J. C **42**, 281 (2005).
[18] S. V. Goloskokov and P. Kroll, Eur. Phys. J. C **50**, 829 (2007).
[19] M. Diehl and W. Kugler, Eur. Phys. J. C **52**, 933 (2007).
[20] S. V. Goloskokov and P. Kroll, Eur. Phys. J. C **53**, 367 (2008).
[21] A. D. Martin *et al.*, Eur. Phys. J. C **63**, 57 (2009).
[22] K. Kumericki and D. Mueller, Nucl. Phys. B **841**, 1 (2010).
[23] M. G. Ryskin, Z. Phys. C **57**, 89 (1993).
[24] S. J. Brodsky *et al.*, Phys. Rev. D **50**, 3134 (1994).
[25] M. Anselmino *et al.*, Eur. Phys. J. A **47**, 35 (2011).
[26] D. Boer *et al.*, arXiv:1108.1713.
[27] A. Accardi *et al.*, arXiv:1110.1031.
[28] D. Y. Ivanov *et al.*, Eur. Phys. J. C **34**, 297 (2004).
[29] M. Vanttinen and L. Mankiewicz, Phys. Lett. B **434**, 141 (1998).
[30] J. Koempel *et al.* (unpublished).
[31] M. Diehl *et al.*, Eur. Phys. J. C **39**, 1 (2005).
[32] S. V. Goloskokov and P. Kroll, Eur. Phys. J. C **59**, 809 (2009).
[33] I. V. Musatov and A. V. Radyushkin, Phys. Rev. D **61**, 074027 (2000).
[34] see, for instance, contribution by M. Diehl in Ref. [26].
[35] S. Meissner, A. Metz, and K. Goeke, Phys. Rev. D **76**, 034002 (2007).
[36] A. V. Efremov *et al.*, Phys. Lett. B **612**, 233 (2005).
[37] M. Anselmino *et al.*, Phys. Rev. D **74**, 094011 (2006).
[38] S. J. Brodsky and S. Gardner, Phys. Lett. B **643**, 22 (2006).
[39] W. Augustiniak (HERMES Collaboration), *DIS2008, London, 2008.*
[40] A. V. Vinnikov, arXiv:hep-ph/0604248.
[41] J. Pumplin *et al.*, J. High Energy Phys. 07 (2002) 012.